ELSEVIER

Polymer 42 (2001) 4253–4260

polymer

www.elsevier.nl/locate/polymer

The structure of poly(di-*n*-propylsilylenemethylene)

S.-Y. Park[a,b], L.V. Interrante[c], B.L. Farmer[b,*]

[a]*Department of Materials Science and Engineering, University of Virginia, Charlottesville, VA 22903-2442, USA*
[b]*Air Force Research Laboratory, Materials and Manufacturing Directorate, Wright-Patterson Air Force Base, OH 45433-7750, USA*
[c]*Department of Chemistry, Rensselaer Polytechnic Institute, Troy, NY 12180-3590, USA*

Received 8 February 2000; received in revised form 9 October 2000; accepted 9 October 2000

Abstract

The structure of poly(di-*n*-propylsilylenemethylene) (PDPrSM) has been studied by X-ray diffraction, electron diffraction and molecular modeling. The fiber X-ray data and the electron diffraction pattern of single crystals show that PDPrSM has triclinic symmetry with unit cell parameters $a = 10.52$ Å, $b = 8.66$ Å, $c = 4.86$ Å, $\alpha = 78.4°$, $\beta = 100.0°$ and $\gamma = 98.2°$. The fiber repeat, 4.86 Å, indicates an all-*gauche* conformation in the main chain, giving a 4_1 helical structure. *Ab initio* and semi-empirical energy calculations show that with attachment of *n*-alkyl side chains an all-*gauche* conformation for the main chain gives the lowest energy. This is in contrast to the unsubstituted polymer, poly(silaethylene), which has a minimum energy for the all-*trans* conformation. The all-*gauche* conformation of the main chain of PDPrSM relieves the steric hindrance between side chains found in the all-*trans* conformation.

Keywords: Poly(di-*n*-propylsilylenemethylene); X-ray diffraction; Conformation

1. Introduction

Polysilylenemethylenes (PSMs, $[SiRR'CH_2]_n$) have recently attracted increasing attention as precursors to silicon carbide fibers [1–3]. Among the potential advantages that this class of polymers may offer compared to other inorganic/organic hybrid polymers are a combination of low T_g, high synthetic versatility (similar to that of polyphosphazenes and polysiloxanes) and good chemical stability (similar to that of the polyolefins) [1–8]. Only the crystal structure of polysilaethylene (PSE) [9] has thus far been reported.

A related family of hybrid polymer, the polysilanes, shows a variety of structures in which the crystalline backbone conformation depends on side chain length [10–16]. The most studied polymer of this family, poly(di-*n*-hexylsilane) (PdnHS) adopts an all-*trans* backbone conformation at room temperature, and transforms to a conformationally disordered state above a transition at 41°C [16]. Polymers with somewhat shorter side chains, poly(di-*n*-pentylsilane) and poly(di-*n*-butylsilane), adopt a 7_3 helical backbone conformation in the solid state [12,17]. Polymers with still shorter side chains, poly(dimethylsilane), poly(diethylsilane) and poly(di-*n*-propylsilane), are again all-*trans* [10,11]. Polymers with somewhat longer side chains, poly(di-*n*-heptylsilane) and poly(di-*n*-octylsilane), have an all-*trans* backbone conformation [14]. Molecular modeling calculations show that both the 7_3 helical and planar zigzag conformations are low-energy conformations for polysilanes, with the helical form being slightly lower in energy [18].

For polysilylenemethylenes, the unsubstituted polymer, PSE, was found to adopt a planar zigzag conformation in the solid state, packing in a unit cell having dimensions $a = 5.70$ Å, $b = 8.75$ Å, c (fiber axis) $= 3.25$ Å and $\gamma = 97.6°$ [9]. The likely effect of *n*-alkyl side chains on the conformation and packing is not obvious. The attachment of two *n*-alkyl side chains on each silicon atom of the backbone may change the conformation because of steric crowding. (The bond length of the Si–Si bond is 2.35 Å in polysilane while that of the Si–C bond is 1.89 Å in the PSMs.) On the other hand, in PSMs only half of the backbone atoms — the silicons — have side chains attached.

In this paper, we report the structure of poly(di-*n*-propylsilylenemethylene), PDPrSM, one of the PSMs. The unit cell dimensions and backbone conformation of PDPrSM have been determined using X-ray and electron diffraction data. Conformational energies have been calculated using *Ab initio* and semi-empirical methods.

2. Experiment

Fiber specimens for X-ray work were prepared by drawing isotropic melts on a glass slide at 80°C with tweezers.

* Corresponding author. Tel.: +1-937-255-9209; fax: +1-937-255-9157.
E-mail address: barry.farmer@afrl.af.mil (B.L. Farmer).

0032-3861/01/$ - see front matter
PII: S0032-3861(00)00766-7

Wide-angle X-ray patterns were recorded on both Kodak Direct Exposure film and phosphor image plates (Molecular Dynamics©) using a Statton camera. Monochromated CuKα radiation was obtained from a Rigaku rotating anode X-ray generator operated at 50 kV and 150 mA. The sample-to-film distance (about 50 mm) was calibrated by SiO_2 powders.

Samples suitable for transmission electron microscopy (TEM) and electron diffraction (ED) were prepared by casting thin films on carbon-coated glass cover slides. A drop of 0.05 wt.% solution of the polymer in toluene was evaporated, melted and crystallized at the desired temperature in a Mettler hot stage. The samples were shadowed with Pt/C (at ~15° incidence angle) or decorated with gold at normal incidence. They were then floated on water (sometimes with the help of poly(acrylic acid)) and mounted on copper grids. Electron diffraction patterns were obtained using a Philips CM-200 TEM equipped with a cooling stage and operating in selected area mode under low-irradiation conditions. To minimize the effects of radiation damage, ED patterns were obtained by searching the samples for suitable patterns and then recording them immediately. (Samples became cross-linked upon exposure, as is the case for other crystalline polymers.) The sample was also tilted to obtain ED patterns from different zones. The macroscopic structure of the polymer was observed using an optical microscope (Leitz Ortholux) with crossed polarizing filters.

The conformational energies were calculated with *ab initio* and semi-empirical methods using the SPARTAN® [19] program. *Ab initio* calculations were made at the Hartree–Fock, 6-31G** level. The AM1 Hamiltonian was employed in the semi-empirical method. Energy minimization was carried out by fixing the backbone torsion angles at the desired value and then allowing all other geometric parameters to be optimized. The conformational energies of $CH_3SiH_2CH_2SiH_3$ and $SiH_3CH_2SiH_2CH_2SiH_3$ were calculated at 10° increments of the torsion angle using the *ab initio* method. The energies of $HCH_2[SiR_2CH_2]_4SiR_2H$ (R = H, $-CH_3$, $-CH_2CH_3$, or $-CH_2CH_2CH_3$) were calculated at selected backbone conformations using the semi-empirical method. The Si–C bond length was fixed at 1.89 Å. The Si–C–Si and C–Si–C bond angles in the main chain were fixed to 116°. The torsion angle for a *cis* conformation was defined as 0°.

3. Results and discussion

3.1. X-ray diffraction

Fig. 1 shows the fiber X-ray pattern of PDPrSM. The observed *d*-spacings are listed in Table 1. Ten sharp reflections on the equator were observed, indicating good lateral packing between chains. All equatorial *hk*0 reflections can be indexed with reciprocal unit cell parameters of

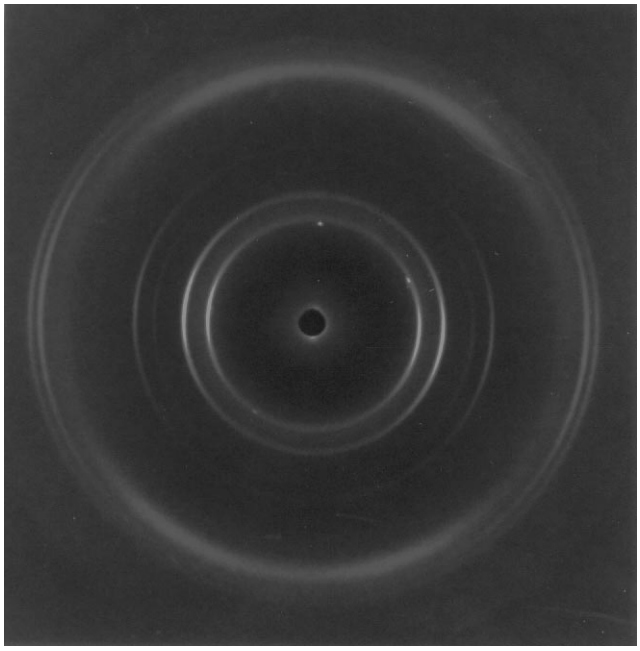

Fig. 1. The fiber X-ray pattern of PDPSM (vertical direction is fiber direction).

Table 1
The observed and calculated *d*-spacings and their indices based on unit cell parameters, $a = 10.52$ Å, $b = 8.66$ Å, $c = 4.86$ Å, $\alpha = 78.4°$, $\beta = 100.0°$ and $\gamma = 98.2°$

h	*k*	*l*	d_o	d_c
1	0	0	10.30	10.30
0	1	0	8.43	8.43
−1	1	0	6.91	6.91
1	1	0	6.19	6.19
2	1	0	4.18	4.19
−1	2	0	4.07	4.06
3	0	0	3.44	3.43
−1	3	0	2.79	2.79
0	3	0		2.81
3	2	0	2.53	2.53
−1	4	0		2.54
−1	1	1	4.46	4.45
0	1	1		4.47
−1	−1	1	3.68	3.68
−2	−1	1	3.19	3.19
−2	2	1		3.20
0	−2	1	2.92	2.89
1	−2	1	2.77	2.77
−2	3	1	2.56	2.55
3	−1	1	2.46	2.46
−4	1	1		2.46
−4	0	1	2.38	2.42
2	−3	1	2.07	2.07
4	−1	1		2.07
0	4	1		2.07
−1	−1	2	2.18	2.17
0	−1	2		2.17

Table 2
The calculated fiber repeat distances for various possible conformations (the bond angles for C–Si–C and Si–C–Si were taken as 116° and the Si–C bond length was 1.89 Å)

Conformation[a]				Repeat distance (Å)
T	*T*	*T*	*T*	3.17
T	*G*	*T*	*G′*	5.67
G	*G*	*G*	*G*	4.90
G	*G′*	*G*	*G′*	None
C	*T*	*C*	*T*	5.43

[a] *T*: *trans* (180°); *G*: *gauche* (68°); *G′*: *gauche′* (−68°); *C*: *cis* (0°).

$a^* = 1/10.30$ Å^{-1}, $b^* = 1/8.43$ Å^{-1} and $\gamma^* = 83.6°$. The observed and calculated *d*-spacings (based on the proposed two-dimensional unit cell dimensions) are in good agreement, indicating the unit cell is either monoclinic or triclinic. The full determination of the unit cell depends on indexing reflections having $l \neq 0$.

Reflections on the first layer line are more diffuse than those on the equator. A reflection at $d = 2.18$ Å on the second layer line is also rather diffuse. The diffuseness of these reflections indicates either smaller crystal size in the chain direction than in the lateral directions or considerable disorder in the chain direction, or both. The first reflection on the first layer line ($d = 4.46$ Å) is strong and located off the meridian, requiring that the fiber repeat be more than 4.46 Å. The fiber repeat distance calculated from the layer line separation is 4.86 ± 0.05 Å. Table 2 shows the calculated fiber repeat distances for various backbone conformations. The observed value agrees well with that of the all-*gauche* conformation. (The torsion angle of 68° was used in order to achieve a periodic structure in the all-*gauche* conformation. As discussed later, this value corresponds to an energy minimum.) Fig. 2 shows the projection along the chain axis of the possible conformations of PSE. The all-*gauche* conformation gives a 4_1 helical structure, with the exact structure depending on the Si–C–Si and C–Si–C bond angles.

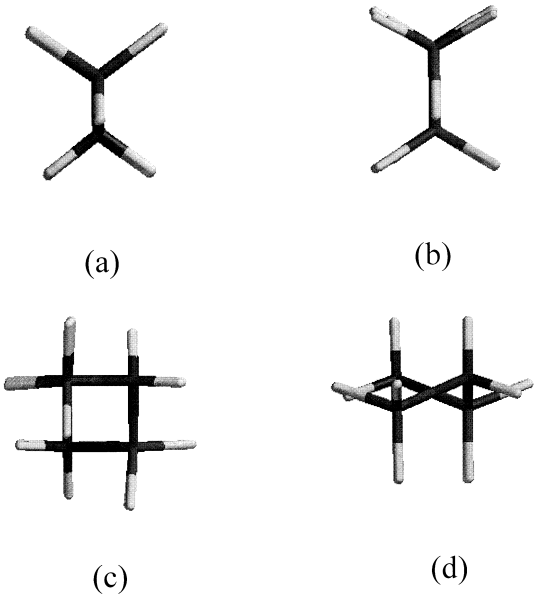

Fig. 2. Projections along the chain axis of PSE for different conformations: (a) *TTTT*; (b) *TCTC*; (c) *GGGG*; and (d) *TGTG′*.

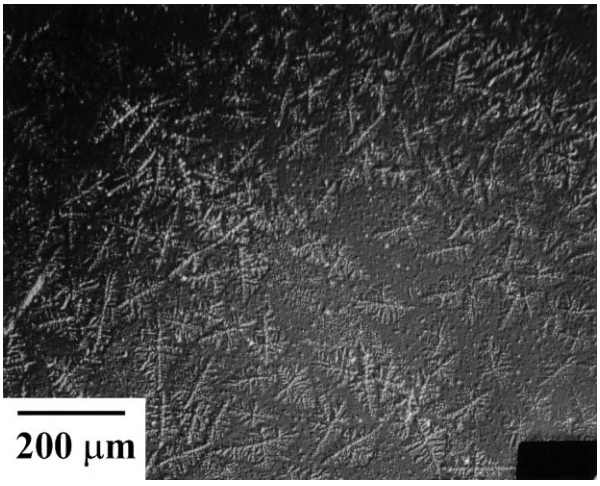

Fig. 3. Polarized optical micrograph of single crystals of PDPSM under crossed polarizing filters.

3.2. Unit cell determination

Fig. 3 shows a polarized optical micrograph of dendritic single crystals grown on a glass slide. Fig. 4 shows the electron diffraction pattern from a single crystal obtained with the electron beam normal to the crystal lamellar surface. The *d*-spacing of the first strong diffraction spot on the horizontal axis is 10.3 Å, corresponding to the first equatorial reflection in the fiber pattern. The *d*-spacing of the first strong diffraction spot in the near-vertical direction

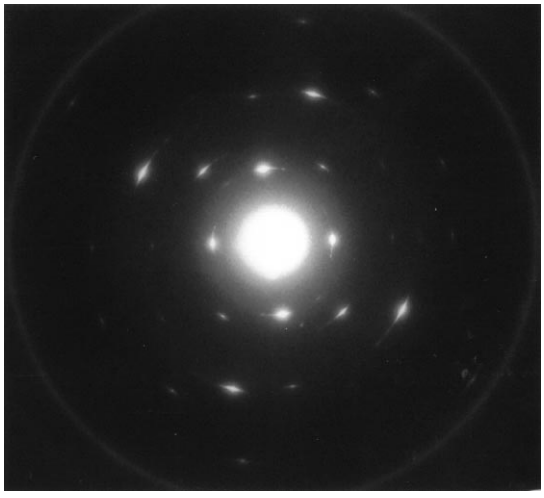

Fig. 4. *hk*0 electron diffraction pattern of a PDPrSM single crystal (a^* is in the equator and b^* is near the meridian).

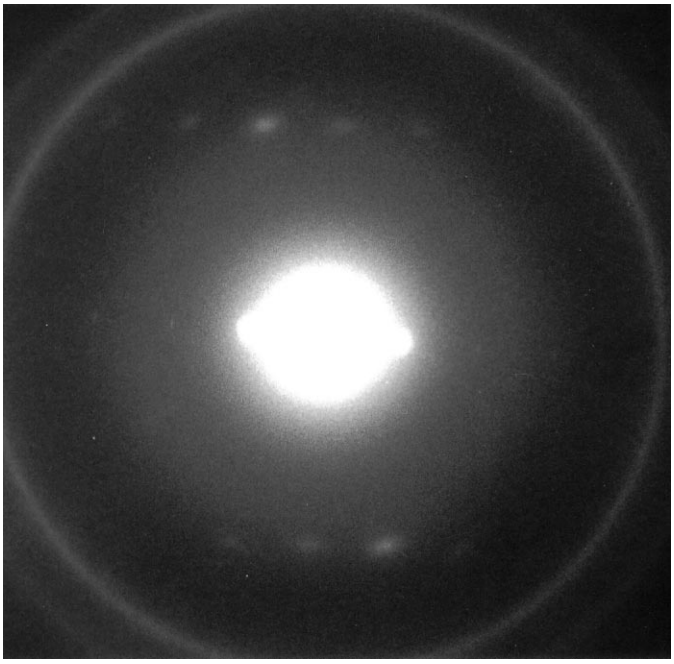

Fig. 5. Electron diffraction pattern for a sample rotated by ~40° from normal to the lamella (the tilt axis is in the plane).

is 8.41 Å, corresponding to the second equatorial reflection in the fiber pattern. These two reflections can be indexed as 100 and 010, respectively. The angle between 100 and 010, γ^*, is 84.5°, nearly the same value obtained from indexing the 10 *hk*0 reflections of the fiber pattern. Thus the electron diffraction pattern consists of *hk*0 reflections, indicating that the molecular chain axis is perpendicular to the lamellar surface. Two-dimensional reciprocal lattice parameters $a^* = 1/10.3$ Å^{-1}, $b^* = 1/8.43$ Å^{-1} and $\gamma^* = 83.6°$ can be obtained from the electron diffraction pattern. These are essentially the same as those from the *hk*0 reflections of the fiber pattern.

Determination of the full three-dimensional unit cell is dependent on locating the c^* vector in the reciprocal lattice. The c^* vector, in general, can be expressed as [*x*,*y*,1/4.86] where 4.86 Å is the fiber repeat distance (*c* unit cell parameter in real space). In order to determine the values of *x* and *y*, more than two *hk*1 reflections must be located and indexed.

Fig. 5 shows the electron diffraction pattern for a sample tilted by ~40° from the normal to the crystal lamellar surface about the horizontal axis (a^*) of Fig. 4. The series of equally spaced (separated by a^*) reflections in the horizontal direction can be indexed as *h*00. Three additional reflections at *d*-spacings of 3.15, 3.64 and 3.80 Å lie on a parallel horizontal line. These reflections correspond to the reflections at 3.19 and 3.68 Å on the first layer line of the X-ray fiber pattern. Thus, these three reflections in the tilted ED pattern can be indexed as $-2k1$, $-1k1$ and $0k1$. This allows c^* to be located. The reciprocal lattice parameters a^*, b^* and c^* can be converted to real-space parameters $a = 10.52$ Å, $b = 8.66$ Å, $c = 4.86$ Å, $\alpha = 78.4°$, $\beta = 100.0°$ and $\gamma = 98.2°$. The measured and calculated *d*-spacings and their indices are listed in Table 1. All observed *d*-spacings are in good agreement with the calculated *d*-spacings, with an average discrepancy for the 19 reflections of ±0.007 Å. The calculated density for two helical repeat units in the unit cell is 1.000 g/cm^3, typical of those measured for other silicon–carbon polymers such as poly(di-*n*-alkylsilanes) [14].

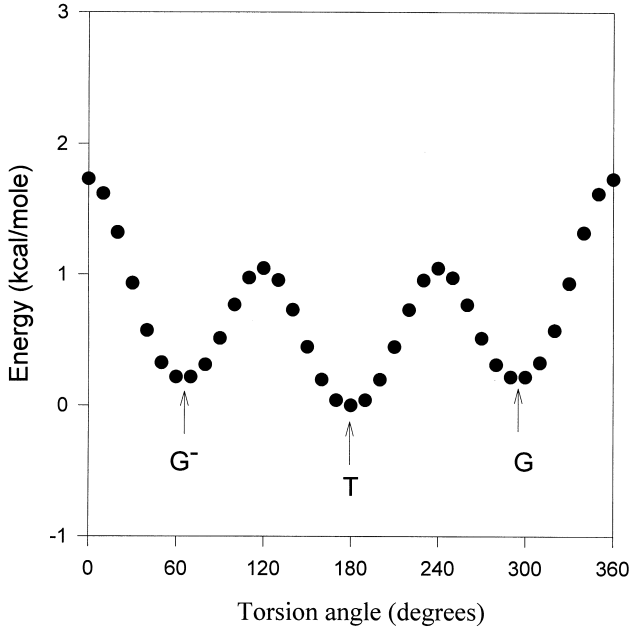

Fig. 6. *Ab initio* energy of $CH_3SiH_2CH_2SiH_3$ *versus* torsion angle (C–Si–C–Si).

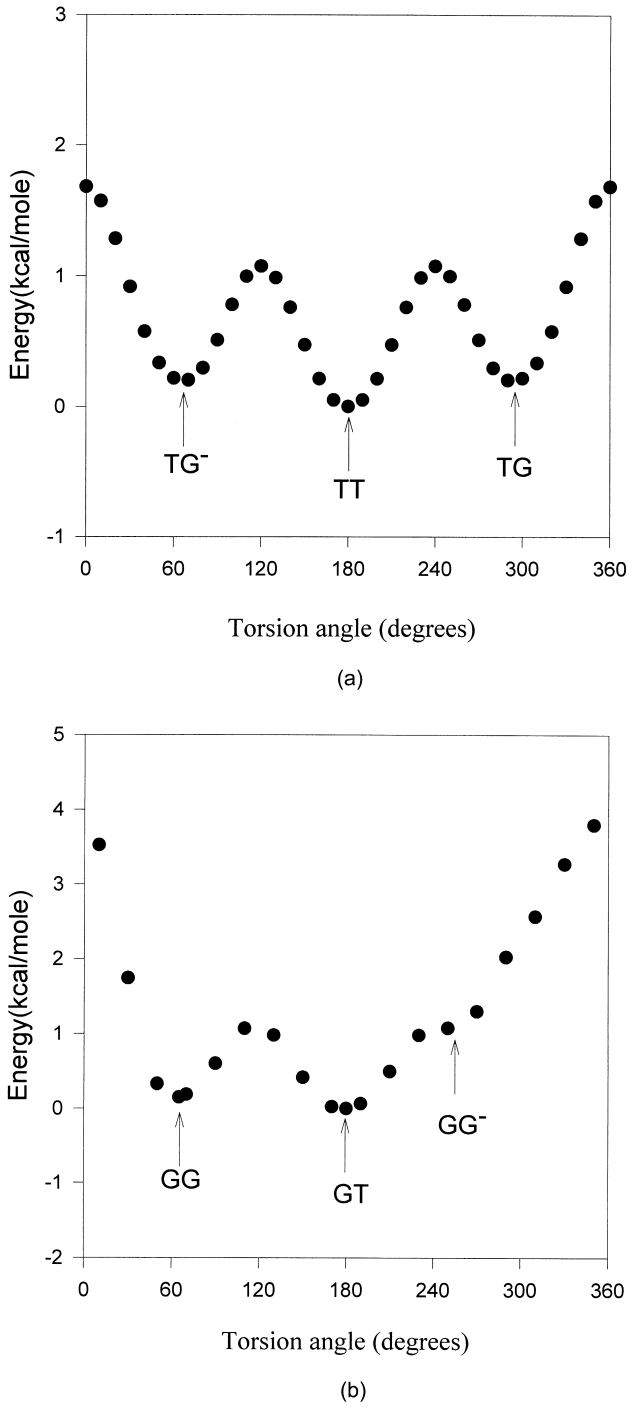

Fig. 7. *Ab initio* energy of $SiH_3CH_2SiH_2CH_2SiH_3$ *versus* torsion angle when the torsion angle of Si–C–Si–C was fixed at: (a) 180° and (b) 68°.

3.3. Energy calculations

The observed fiber repeat distance, 4.86 Å, indicates that the main polymer chain has an all-*gauche* conformation. This is in contrast to the unsubstituted polymer, PSE, which has an all-*trans* conformation. Fig. 6 shows the relative energy as a function of torsion angles for a $CH_3SiH_2CH_2SiH_3$ molecule, computed at the *ab initio* level. The minimum energy occurs for the *trans* conformation, consistent with X-ray results for PSE. The *gauche* conformation at ~68° is also a relative energy minimum and is only 0.22 kcal/mol higher. This compares to a difference of 0.99 kcal/mol for the corresponding hydrocarbon, *n*-butane, $CH_3CH_2CH_2CH_3$. A *gauche* conformation in the backbone of PSMs may be energetically feasible.

Table 3
Conformational energies of $HSiH_2CH_2SiH_2CH_2SiH_3$ calculated at the *ab initio* HF, 6-31G** level ($\phi_1 = Si–C–Si–C$, $\phi_2 = C–Si–C–Si$)

Conformation		Relative energy (kcal/mole)
$\phi_1 = T$	$\phi_2 = G$	
TT		0
TG		0.20
TC		1.68
	GT	0.20
	GG	0.34
	GG′	1.21

Fig. 7a and b shows the relative energy (*ab initio* method) versus torsion angle for $SiH_3CH_2SiH_2CH_2SiH_3$ which contains two backbone torsion angles, Si–C–Si–C and C–Si–C–Si. In Fig. 7a, the Si–C–Si–C torsion angle was fixed at 180° (*trans*) while the other torsion angle was rotated incrementally. There are three minima: *trans–trans* (*TT*), *trans–gauche* (*TG*) and *trans–gauche′* (*TG′*). *TT* has the lowest energy while *TG* and *TG′* have the same, slightly higher energy. In Fig. 7b, the Si–C–Si–C torsion angle was fixed at 68° (*gauche*). Again there are three energy minima: *gauche–gauche* (*GG*), *gauche–trans* (*GT*) and *gauche–gauche′* (*GG′*). The energies of *GG* and *GT* are very similar, while *GG′* has higher energy due to the pentane effect. The energy values are summarized in Table 3. *TT* has the lowest energy, while *TG* and *GG* have similar energies (only 0.20 and 0.34 kcal/mol higher, respectively). *TC* has the highest energy and is not a relative minimum. These energy differences are small compared to polyethylene, suggesting the –Si–C– chain may be considerably more flexible.

Because of computational limitations, semi-empirical methods were employed to study the conformation of longer, substituted PSMs. The relative energies of $HCH_2[SiR_2CH_2]_4SiR_2H$ with different side chains (from R = H to R = $CH_2CH_2CH_3$) are listed in Table 4. The minimum energy of the unsubstituted polymer, PSE (R = H) now occurs for the all-*gauche* conformation, in contrast to

Table 4
The relative energies of $HCH_2[SiR_2CH_2]_4SiR_2H$ (R = H, CH_3, CH_2CH_3 or $CH_2CH_2CH_3$) using the semi-empirical method (the all-*gauche* energy has been assigned a value of 0 in each column)

Conformation				Relative energy (kcal/mol)			
				R = H	R = CH_3	R = CH_2CH_3	R = $CH_2CH_2CH_3$
T	*T*	*T*	*T*	3.1	14.2	30.4	43.9
T	*G*	*T*	*G′*	1.3	2.7	5.7	5.8
G	*G*	*G*	*G*	0	0	0	0
T	*C*	*T*	*C*	8.4	3.4	6.8	6.8

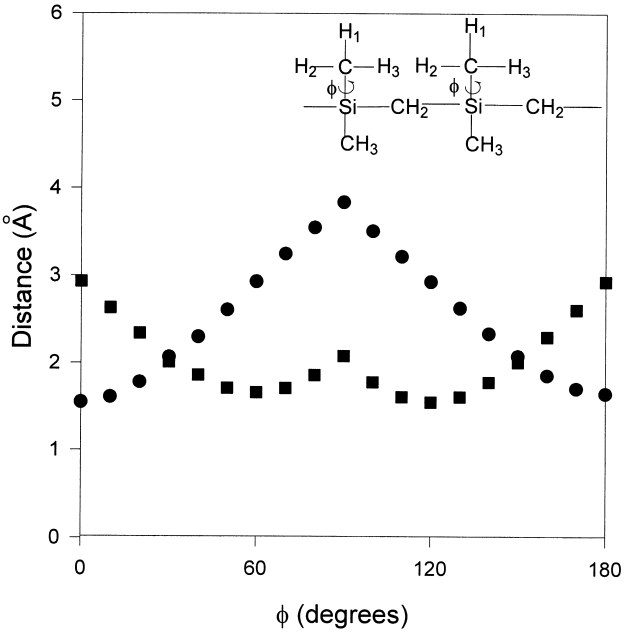

Fig. 8. The distance between hydrogens of side chains in poly(dimethylsilylenemethylene) (PdMSM) in an all-*trans* backbone conformation (■, distance between H_1 and H_3; ●, distance between H_2 and H_3).

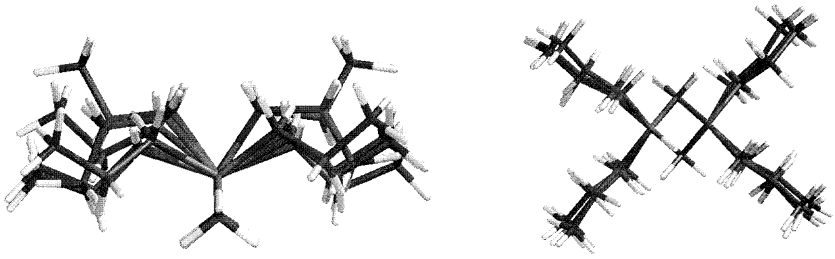

(a) (b)

Fig. 9. The energy minimized structures for $HCH_2[SiR_2CH_2]_4SiR_2H$ ($R = CH_2CH_2CH_3$) when the backbone conformation is: (a) all-*trans* and (b) all-*gauche*.

ab initio results which gave a lower energy for the all-*trans* conformation. (This difference is not due to the longer molecule used for the semi-empirical calculations. The semi-empirical minimum energy for a $CH_3SiH_2CH_2SiH_3$ also occurs for the all-*gauche* conformation.) Nonetheless, the energy differences between conformations of PSE are small. Attaching alkyl side chains dramatically increases the energy for the all-*trans* conformation of the backbone, making the all-*trans* conformation very unlikely. The all-*gauche* conformation is the most stable conformation of symmetrically substituted PSMs.

One reason the PSM backbone adopts an all-*gauche* conformation instead of the all-*trans* conformation seen in some polysilanes is the decrease of bond length from Si–Si (2.34 Å) to Si–C (1.89 Å). This leads to steric hindrance between side chains in the all-*trans* conformation in the PSMs. (There is also steric hindrance in the polysilanes, but the presence of side chains on every backbone atom prevents a *gauche* conformation from providing any steric relief.) Fig. 8 shows the shortest distance between hydrogens of side chains of poly(dimethylsilylenemethylene) (PDMSM) in an all-*trans* backbone conformation. Torsion angles for the side chains were defined as C_1–Si–C_2–H, where C_1 and C_2 are the carbon atoms in the two methyl groups attached to the same silicon atom. At all torsion angles, the shortest distance is less than 2.4 Å, the sum of the van der Waal's radii for two hydrogen atoms.

Longer side chains give still more steric hindrance. Fig. 9a and b shows the energy minimized structures for all-*trans* and all-*gauche* backbone conformations, respectively. For the all-*trans* backbone, it is apparent that the side chains are distorted to reduce steric hindrance. The side chains are not distorted in the all-*gauche* conformation.

4. Conclusions

The structure of PDPrSM has been studied by X-ray diffraction, electron diffraction and molecular modeling. In the X-ray fiber pattern, the reflections on the equator were sharper than those on the first and second layers, indicating good lateral packing. Dendritic single crystals were grown by melt crystallization of thin films. The combination of fiber X-ray data and electron diffraction from single crystals shows that PDPrSM has triclinic symmetry with unit cell parameters $a = 10.52$ Å, $b = 8.66$ Å, $c = 4.86$ Å, $\alpha = 78.4°$, $\beta = 100.0°$ and $\gamma = 98.2°$. The 4.86 Å fiber repeat distance indicates that the backbone conformation is all-*gauche* giving a 4_1 helical structure. *Ab initio* and semi-empirical energy calculations show that attaching *n*-alkyl side chains leads preferentially to an all-*gauche* conformation. Steric hindrance between side chains disfavors the all-*trans* conformation found for the unsubstituted polymer (PSE).

Acknowledgements

We thank Prof. P. Geil for assistance with electron diffraction methods. Support from National Science Foundation through grant DMR-9731345 is gratefully acknowledged.

References

[1] Laine RM, Babonneau F. Chem Mater 1993;5:260.
[2] Seyferth D, Lang H. Organometallics 1991;10:551.
[3] Birot M, Dunogues J-P. J Chem Rev 1995;95:1443.
[4] Mark JE, Allcock HR, West R. Inorganic polymers. New York: Prentice-Hall, 1992 (p. 154).
[5] Bazant V, Chvalovsky V, Rathousky J. Organosilicon compounds. New York: Academic Press, 1965 (p. 47).
[6] Bacque E, Pillot J-P, Birot M, Dunoges J. Macromolecules 1988;21:30.
[7] Habel W, Mayer L, Sartory P. J Organomet Chem 1994;474:63.
[8] Rushkin IL, Interrante LV. Macromolecules 1996;29:3123.
[9] Tsao M-W, Pfeifer K-H, Rabolt JF, Holt DB, Farmer BL, Interrante LV, Shen Q. Macromolecules 1996;29:7130.
[10] Lovinger AJ, Davis DD, Schilling FC, Bovey FA, Padden FA, Zeigler JM. Macromolecules 1991;24:132.
[11] Lovinger AJ, Davis DD, Schilling FC, Bovey FA, Zeigler JM. Polym Commun 1989;30:356.
[12] Schilling FC, Lovinger AJ, Zeigler JM, Davis DD, Bovey FA. Macromolecules 1989;22:3055.

[13] Lovinger AJ, Schilling FC, Bovey FA, Zeigler JM. Macromolecules 1986;19:2557.
[14] KariKari EK, Greso AJ, Farmer BL, Miller RD, Rabolt JF. Macromolecules 1993;26:3937.
[15] Kuzumany H, Rabolt JF, Farmer BL, Miller RD. J Chem Phys 1986;85:7413.
[16] Patnaik SS, Farmer BL. Polymer 1992;33:4443.
[17] Miller RD, Farmer BL, Fleming W, Sooriyakumaran R, Rabolt JF. J Am Chem Soc 1987;109:2509.
[18] Farmer BL, Rabolt JF, Miller RD. Macromolecules 1987;20:1167.
[19] Spartan, Version 4, Irvine, CA: Wave function, Inc., 1997.